

Phonon softening in Ni-Mn-Ga alloys

Lluís Mañosa and Antoni Planes

Departament d'Estructura i Constituents de la Matèria, Universitat de Barcelona, Avinguda Diagonal 647, Facultat de Física, E-08028 Barcelona, Catalonia, Spain

J. Zarestky, T. Lograsso, D. L. Schlagel, and C. Stassis

Ames Laboratory and Department of Physics and Astronomy, Iowa State University, Ames, Iowa 50011

(Received 24 July 2000; revised manuscript received 12 January 2001; published 21 June 2001)

The TA_2 phonon dispersion curves of Ni-Mn-Ga alloys with different compositions which transform to different martensitic structures have been measured over a broad temperature range covering both paramagnetic and ferromagnetic phases. The branches show an anomaly (dip) at a wave number that depends on the particular martensitic structure, and there is softening of these anomalous phonons with decreasing temperature. This softening is enhanced below the Curie point, as a consequence of spin-phonon coupling. This effect is stronger for systems with higher electronic concentration.

DOI: 10.1103/PhysRevB.64.024305

PACS number(s): 63.20.-e, 81.30.Kf, 64.70.Kb

I. INTRODUCTION

Ni-Mn-Ga alloys close to the stoichiometric composition have drawn the attention of many scientists in recent years. The combination of ferromagnetic and martensitic transitions confers on this alloy unique magnetomechanical properties.¹ The large recoverable deformations (magnetic shape-memory effect) induced by the application of a magnetic field^{2,3} open up the possibility of building magnetic actuators much more powerful than those based on the standard magnetostrictive effect.

From a fundamental point of view, this alloy exhibits singular lattice-dynamical behavior. Pronounced softening of the TA_2 branch phonons around $\xi = (\frac{1}{3}, \frac{1}{3}, 0)$ has been reported on cooling.^{4,5} The shear elastic constants also decrease on cooling.^{6,7} Although elastic constant and phonon softening is a common feature of martensitic alloys,⁸ the degree of softening in Ni-Mn-Ga is much larger than expected. In addition, the pressure dependence of the elastic constants cannot be accounted for by conventional anharmonic theories.⁹ This peculiar behavior is associated with the coupling between magnetic and vibrational degrees of freedom.^{5,10,9} An interesting result is that for certain compositions there is an increase in phonon frequency and in the elastic constants below a given temperature T_I , slightly above the martensitic transition temperature M_s .^{4,7} Such a stiffening is related to the development of an intermediate phase^{4,11} (micromodulated cubic structure) which occurs via a first order phase transition with a very small latent heat.¹⁰

It has been established^{12,1} that the relative stability of the different magnetic and structural phases (including the intermediate micromodulated phase) depends upon the electron concentration (e/a). Different martensitic structures occur on increasing e/a . For low e/a the martensite has been acknowledged to be tetragonal with five-layer modulation and for higher e/a different modulated structures have been reported.¹² The intermediate phase is observed only for e/a values $\lesssim 7.7$.¹ In this paper we present the results of a lattice-dynamical study by neutron scattering on two Ni-Mn-Ga al-

loys with different e/a . The study is complemented with calorimetric, magnetic susceptibility, and x-ray diffraction measurements. In one of the alloys, the martensitic transition temperature is close to the Curie point (high e/a) and in the other one (low e/a) it is far from the Curie point. Results are compared with data from the literature.

II. EXPERIMENTAL DETAILS

Two single crystals were grown at the Ames Laboratory. Appropriate quantities of nickel (99.99% pure), electronic grade gallium (99.999%), and electrolytic manganese (99.9%) were cleaned and arc melted several times under an argon atmosphere. The buttons were then remelted and the alloy drop cast into a copper chill cast mold to ensure compositional homogeneity throughout the ingot. The as-cast ingots were placed in alumina crucibles (approximately 15 mm in diameter) and crystal growth was done in a Bridgman-style refractory metal resistance furnace. The ingots were heated to 1350°C for 1 h to allow homogenization before withdrawing the sample from the heat zone at a rate of 2.0 mm/h. To minimize vaporization of the manganese during crystal growth, the furnace was backfilled to a positive pressure of 6.8×10^5 Pa with purified argon after the chamber and sample had been outgassed at 1350°C under vacuum. Due to the directional nature of the crystal growth and convective mixing forces present in the liquid prior to solidification, significant concentration gradients exist along the length of the ingots. Samples sectioned from the bottom and top of the single crystals provided specimens of different composition. The actual composition of the investigated samples was determined by chemical analysis to be $Ni_{52.0}Mn_{23.0}Ga_{25.0}$ (sample 2, $e/a = 7.56$), and $Ni_{50.5}Mn_{29.5}Ga_{20.0}$ (sample 3, $e/a = 7.71$). The composition gradient for sample 2 was significantly stronger than for sample 3. The rocking curves of these samples show structure representative of slightly misaligned grains which produce a full width at half maximum of $\sim 1^\circ$.

Neutron scattering experiments were carried out on the HB1, HB3, and HB1A (Ames Laboratory PRT) spectrom-

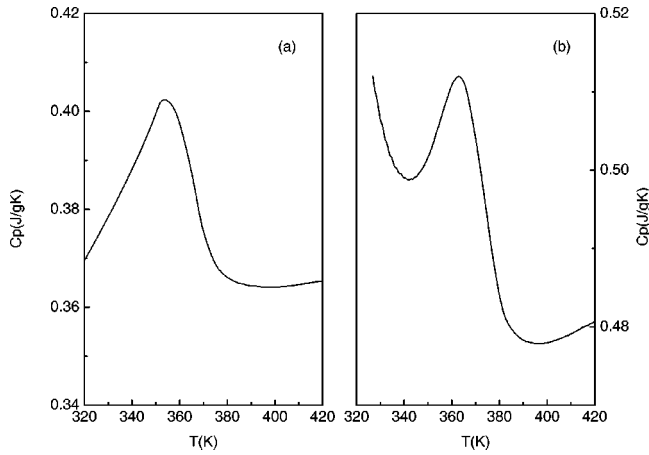


FIG. 1. Specific heat as a function of temperature: (a) sample 2; (b) sample 3.

eters at the High Flux Isotope Reactor (HFIR) of the Oak Ridge National Laboratory. Pyrolytic graphite reflecting from the (002) planes was used as an analyzer. The data were collected either in the constant- \vec{Q} mode (where \vec{Q} is the scattering vector) or at fixed scattered neutron energies of 13.6 and 14.7 meV and at fixed incident neutron energy of 14.7 meV. Typical collimations of 50'-40'-40'-70' and 50'-40'-40'-120' were used. A pyrolytic graphite filter was also used for all measurements. The energy resolution was approximately 0.8 meV.

For measurements below room temperature a standard Displex helium refrigerator was used and for the field measurements an Oxford Instruments cryomagnet was utilized. For the measurements above room temperature a vacuum furnace was used.

From the large crystals, samples for calorimetric and ac susceptibility measurements were cut using a low speed diamond saw. Specific heat measurements were performed in the range 300–500 K using a modulated differential scanning calorimeter (TA Instruments), and differential scanning calorimetry measurements were carried out in the range 80–350 K using a high sensitivity calorimeter specifically designed for the study of solid-solid phase transitions.¹³ Magnetic susceptibility was measured in the range 80–300 K using a commercial ac susceptometer (Lakeshore). Powdered specimens were obtained using a diamond file. The powder, partially amorphized as a result of the filing, was annealed for 7 h at 673 K under an argon atmosphere. X-ray experiments on these powdered samples were performed in a Bragg-Brentano diffractometer equipped with a temperature attachment and a position sensitive detector.

III. EXPERIMENTAL RESULTS AND DISCUSSION

The structural and ferromagnetic transitions were detected by calorimetry on the two crystals investigated. In Fig. 1 we present the temperature dependence of the specific heat showing the λ peak at the Curie point. For sample 3 [Fig. 1(b)] the upward bending below 340 K is caused by the onset of the martensitic transition. Heat flow is shown in Fig. 2. The small peak observed in the thermogram corresponding

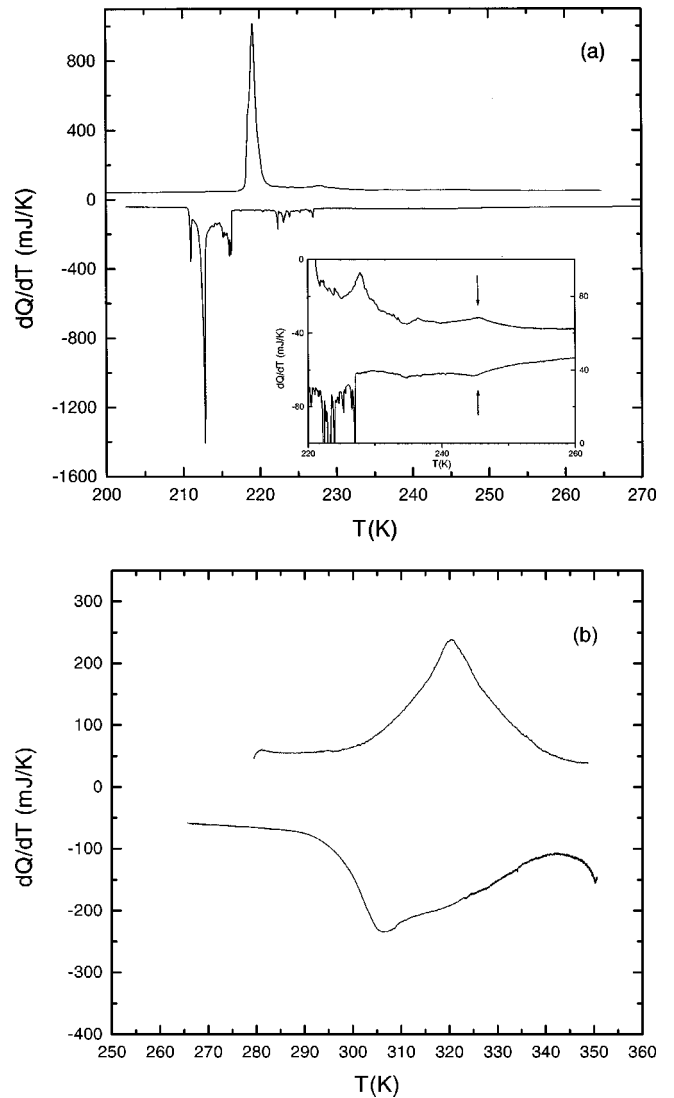


FIG. 2. Thermograms recorded during cooling and heating calorimetric runs: (a) sample 2; (b) sample 3. The inset in (a) shows an enlarged view in a restricted temperature range.

to sample 2 [see the enlarged scale shown in the inset of Fig. 2(a)], indicated by an arrow is likely to be ascribed to the intermediate phase transition. The estimated transition temperatures from calorimetric data are $T_c = 359.5$ K and $M_s = 227$ K for sample 2 and $T_c = 365.5$ K and $M_s = 345$ K for sample 3. The uncertainty in determining M_s for sample 3 is large (around 5 K) since the martensitic transition is very close to the Curie point and the calorimetric baseline is not well defined [see Fig. 2(b)]. Comparison between Figs. 2(a) and 2(b) reveals a markedly different thermal spectrum: the transformation in sample 3 is smoother than that of sample 2. This different kinetic behavior has already been reported in other shape-memory alloys, and has been shown to arise from the different growth mechanisms of the different martensitic structures.¹⁴ Results shown in Fig. 2 suggest that the martensitic structures for the two samples investigated are different. To confirm this suggestion, we have performed x-ray diffraction measurements at low temperature aimed at determining the actual martensitic structure of the studied

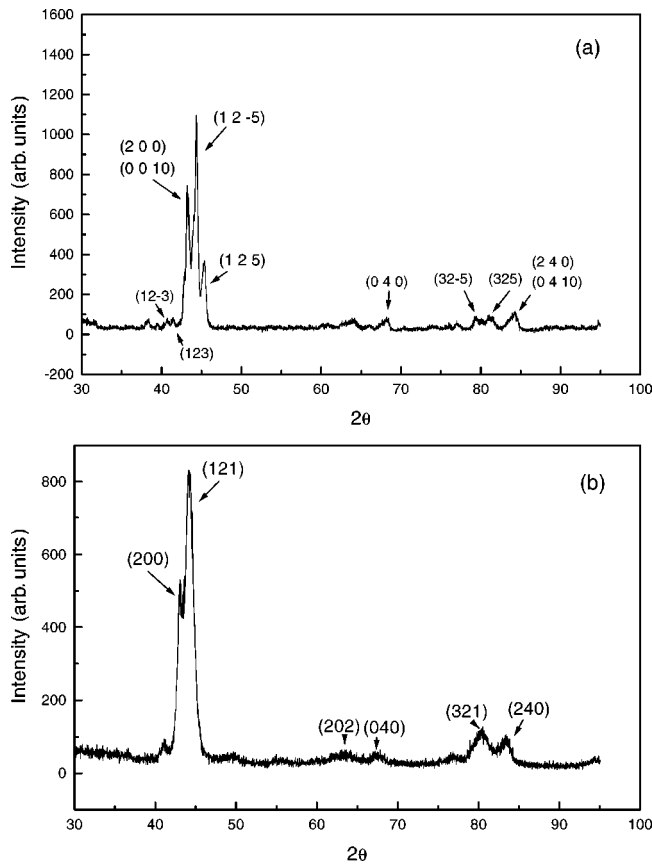


FIG. 3. X-ray diffraction patterns recorded at 193 K on powdered specimens of sample 2 (a) and sample 3 (b).

samples. The diffractograms shown in Figs. 3(a) and 3(b) confirm the different martensitic structures of the two samples. For sample 3, the martensite is tetragonal non-modulated (termed in the literature $3R$, $2M$, or $L1_0$); the lattice parameters are $a=4.2$ Å, $b=5.6$ Å, and $c=4.2$ Å; $\alpha=\beta=\gamma=90^\circ$. A five-layered martensite (termed in the literature $5R$ or $10M$) is obtained for sample 2. The unit cell is monoclinic with the following parameters: $a=4.2$ Å, $b=5.5$ Å, and $c=21$ Å; $\alpha=90^\circ$, $\beta=91^\circ$, $\gamma=90^\circ$.

The structure of the martensite in Ni-based alloys has traditionally been described in terms of a tetragonal unit cell with a shuffling (modulated approach) of the close-packed planes with 5 ($5R$ martensite) or 7 ($7R$ martensite) periodicity. In a different approach, a monoclinic unit cell is used, with different long period stacking of close-packed planes (period stacking approach).¹⁵ A critical comparative analysis of these two approaches for Ni-Mn-Ga has recently been undertaken by Pons *et al.*¹⁶ To distinguish between the two approaches, the angle β between the a and c axes needs to be well determined. From their transmission electron microscopy results, Pons *et al.*¹⁶ established that the seven-layered martensite is monoclinic, but they were not able to distinguish a β angle different from 90° for the five-layered specimen. The results presented here demonstrate that the unit cell for the five-layered martensite is indeed monoclinic ($\beta=91^\circ$) as evidenced by the splitting of the (125) and (12 $\bar{5}$) peaks, and thus it is better described by a $(3\bar{2})_2$ stacking

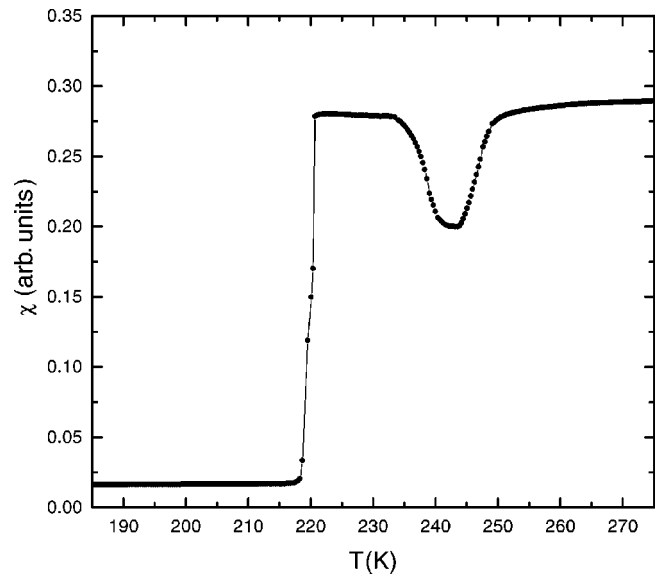


FIG. 4. ac magnetic susceptibility as a function of temperature, for sample 2.

sequence (Zhdanov notation). Even so, the degree of monoclinicity is so small that the use of a modulated tetragonal cell also provides a good description of this structure.

In order to confirm the existence of an intermediate transition toward a micromodulated phase in sample 2, we have performed susceptibility measurements. ac susceptibility is very sensitive to the intermediate phase transition.⁷ Results for an ac field of 10 Oe and a frequency of 66 Hz are shown in Fig. 4. A marked dip is seen at 245 K. This temperature coincides with that of the calorimetric peak and is a clear evidence of the intermediate phase transition. At the martensitic transition there is a sharp decrease in χ , associated with the higher magnetic anisotropy of the martensitic phase.

In Fig. 5(a) we present the temperature dependence of the integrated intensity of the (220) Bragg peak for sample 2. A significant decrease in the intensity occurs at the onset of the martensitic transition. A good correlation exists with macroscopic measurements (calorimetry and susceptibility). The fact that in Fig. 5(a) the transition spreads over a broader temperature range is caused by the composition gradients present in the large crystal of sample 2. As previously mentioned, the composition gradient in sample 3 was much smaller. This is illustrated by Fig. 5(b), which shows the hysteresis loops obtained from the integration of the thermograms recorded on samples cut from the top (continuous line) and bottom (discontinuous line) of the large crystal.

Figure 6 shows the measured TA_2 branch for the two samples, at selected temperatures above the martensitic transition. Overall, the energies are comparable to those reported in other alloys with compositions close to those of the crystals investigated here.^{4,5} Significant phonon softening for those phonons around $\xi=0.3$ is observed on cooling, resulting in a marked dip in the branch which becomes more pronounced as the temperature decreases. For sample 3, such a softening is clearly visible for temperatures below the Curie point. It is interesting to note that the position of the dip is slightly different for the two samples. For sample 2 it is

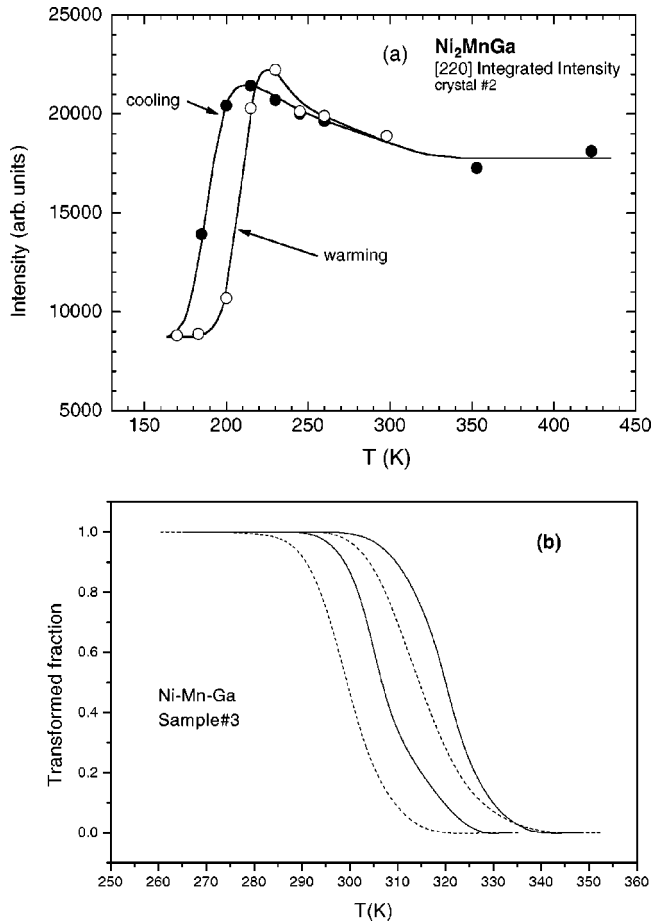


FIG. 5. (a) Integrated intensity of the (220) Bragg peak as a function of temperature, for sample 2. (b) Transformed fraction obtained by integration of the thermograms recorded from samples cut from the top (continuous line) and bottom (discontinuous line) of the large crystal 3.

located at $\xi=0.33$ while for sample 3 it is at $\xi=0.25$. The behavior of sample 2 is similar to that reported by Zheludev *et al.*⁴ This is consistent with the fact that the transition temperatures for sample 2 and that of Ref. 4 are close, which indicates that the compositions of the two samples are not significantly different.¹⁷ Moreover, the two samples transform to the same martensitic structure (five-layer modulation). For sample 3, the dip is less marked (it is broader and not very deep) and resembles that reported very recently for a sample transforming above room temperature (close to the Curie point).¹⁸ While at low temperature the dip is located around $\xi=0.25$, the maximum softening occurs for those phonons at $\xi=0.33$.

The composition dependence of the location of the dip in the TA_2 branch parallels the behavior reported for Ni-Al alloys.¹⁹ In that system, for the alloy transforming to the $3R$ structure, the dip was broad and centered at $\xi=0.14$, which is close to the wave number obtained for Ni-Mn-Ga (sample 3) when $L2_1$ atomic order is considered. As argued for Ni-Al, the phonon dip for samples transforming to $3R$ never gets deep enough and the strain energy associated with this wave vector is not sufficiently large to induce a modulation in the low temperature martensite. Electron-phonon coupling

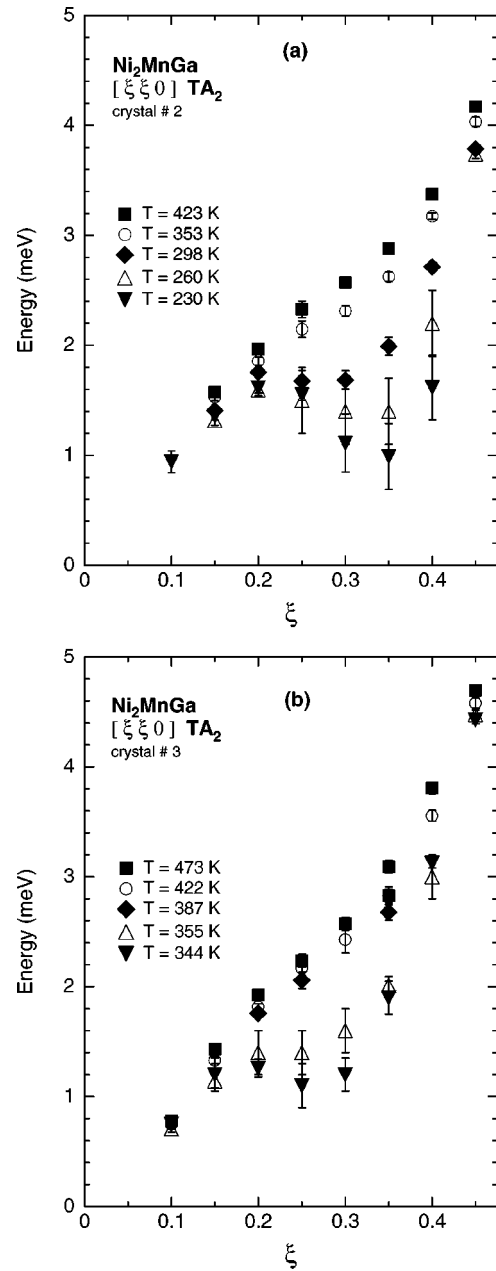


FIG. 6. TA_2 phonon dispersion curves of (a) sample 2 and (b) sample 3 at selected temperatures above the martensitic transition.

is at the origin of the anomalous phonon behavior of Ni-Al alloys, and a composition dependency of the anomaly in the TA_2 branch has been obtained from detailed first principles calculations.²⁰ For Ni-Mn-Ga, it has been argued¹¹ that the origin of phonon anomalies could be the same. The composition dependence reported in the present paper supports this idea. *Ab initio* calculations for off-stoichiometric alloys would provide valuable information to elucidate the physical origin of phonon anomalies in this alloy system. However, in Ni-Mn-Ga, the contribution from magnetism (spin-phonon coupling) plays a relevant role, as will be shown in the following. This should be taken into account in any calculation of the phonon branches in these alloys.

The degree of softening is quantified by the temperature

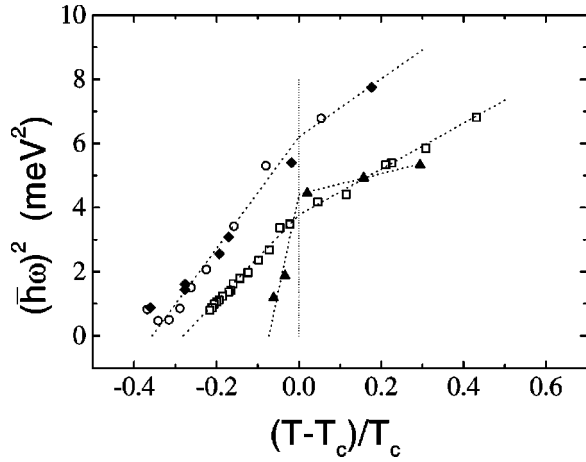


FIG. 7. Energy of the phonon at the dip of the TA_2 branch, as a function of the reduced temperature. T_c is the Curie temperature. Diamonds correspond to sample 2 and triangles to sample 3. Circles are from Ref. 4 and squares from Ref. 5.

dependence of the energy of the phonon at the dip of the branch. This dependence is plotted in Fig. 7 as a function of the reduced temperature. For comparison we have also plotted data for other Ni-Mn-Ga crystals. Linear behavior is observed for all samples but with a different slope of the ω^2 vs T curves in paramagnetic and ferromagnetic phases. As already mentioned, sample 2 behaves similarly to that investigated by Zheludev *et al.*⁴ In particular, notice that, using the reduced temperature, data points of the two samples collapse (within experimental errors) onto a single curve. Stiffening of the anomalous phonon is observed at temperatures slightly above the martensitic transition.⁴ Figure 7 shows that the degree of phonon softening is enhanced at the Curie point. Such enhancement is different for the different samples.

The intermediate phase has not been observed for all Ni-Mn-Ga alloys. It has been suggested^{10,21} that the occurrence of the intermediate transition is associated with a relatively strong coupling between magnetic and vibrational degrees of freedom. This is experimentally supported by the fact that the intermediate phase has been observed only in samples with a martensitic transition temperature well below the Curie point.¹ In Fig. 8 we have plotted the slope of the $(\hbar\omega)^2$ vs T curves in both paramagnetic and ferromagnetic phases, as a function of the temperature gap between the ferromagnetic and martensitic transitions. The values in the paramagnetic phase are similar and close to that measured in Ni-Al,²² indicated in the figure by a dotted line. For all samples the slope in the ferromagnetic is larger than in the paramagnetic phase. This difference is almost one order of magnitude larger for the sample with a small gap between the two transitions.

Recent Monte Carlo simulations by Castán *et al.*²¹ suggest that two conditions have to be fulfilled for a given alloy to exhibit an intermediate phase transition: on the one hand a large spin-phonon coupling is necessary, but also the energy of the soft phonon has to be small enough to enable the instability to develop. Analysis of the data given in Fig. 7 within this theory indicates that although $d(\hbar\omega)^2/dT$ is larger for sample 3 (this could be indicative of a stronger spin-phonon coupling), the occurrence of the martensitic

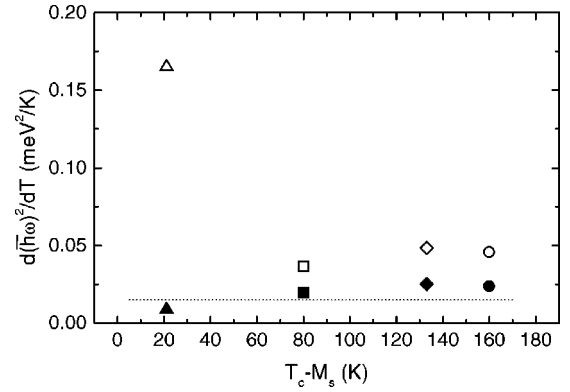


FIG. 8. Slope of the $(\hbar\omega)^2$ vs temperature curves for different Ni-Mn-Ga crystals as a function of the temperature gap between ferromagnetic and martensitic transitions. Diamonds correspond to sample 2, triangles to sample 3, circles to sample of Ref. 4, and squares to sample of Ref. 5. Solid symbols stand for values above the Curie point and open symbols below the Curie point. The dashed line indicates the value for Ni-Al (from Ref. 22).

transition at high temperatures prevents the frequency of the soft phonon from reaching a value small enough to enable development of the intermediate phase. The same reasoning also holds for the sample investigated by Stühr *et al.*,⁵ for which $T_c - M_s$ is relatively small. By contrast, the sample investigated by Zheludev *et al.*⁴ has a lower martensitic transition, and this enables the phonon frequency to reach very low values (see Fig. 6) and the intermediate phase can develop. Sample 2 of the present work is a limiting case. For this sample the intermediate and martensitic transition temperatures are expected to be extremely close (see the phase diagram in Ref. 1). Within the errors, according to Fig. 7 the martensitic transition takes place when the phonon energy is around 1 meV for all samples. For those alloys with a pre-martensitic transition, the value of $(\hbar\omega)$ at T_I is well below 1 meV and upon further cooling it rises to reach the value at which the martensitic transition occurs.

Finally, we have measured the TA_2 branch of sample 2 under the application of a 6.5 T magnetic field. Preliminary results indicate that the effect of the field, if any, is very small (changes in phonon frequencies are smaller than the experimental errors). However, a small but systematic increase of the energies of the soft phonons seems to occur in all cases. That is, application of a magnetic field slightly reduces the depth of the dip in the phonon branch. This behavior parallels that of elastic constants, which also increase with increasing magnetic field.⁹ The relative increase in the elastic constants ($\sim 1\%$) up to saturating magnetic field is of the same order of magnitude as the relative increase in the frequencies of the anomalous phonon ($\Delta\omega/\omega \sim 1\%$ for $\xi = 0.33$). Should an increase in the frequencies of the soft phonons exist, it would be consistent with macroscopic measurements that report a decrease of the intermediate transition temperature with increasing magnetic field.^{10,23}

IV. SUMMARY AND CONCLUSIONS

We have measured the TA_2 phonon dispersion curves for two Ni-Mn-Ga alloys with different electron to atom ratios. For low e/a the martensitic structure is monoclinic with a

stacking periodicity of $(3\bar{2})_2$ while for high e/a the martensite is tetragonal nonmodulated. On cooling, a significant dip develops. The position of this dip depends on composition. In all cases, the softening of these anomalous phonons is enhanced when the sample orders ferromagnetically. The degree of softening has been quantified by the slope of the energy vs T curves. In the paramagnetic phase this slope is similar for all alloys within experimental errors, and is of the same order of magnitude as that of nonmagnetic alloys (Ni-Al). In the ferromagnetic state the softening is larger, and there is a significant change for samples with large e/a .

ACKNOWLEDGMENTS

This work received financial support from the CICYT (Spain), Project No. MAT98-0315, and from the CIRIT (Catalonia), Project No. 2000SGR00025. X-ray diffraction experiments were performed at Serveis Científic Tècnics (Universitat de Barcelona) with the help of J. Bassa. Ames Laboratory is operated for the U.S. Department of Energy by Iowa State University under Contract No. W-7405-Eng-82. The work at Ames was supported by the Director for Energy Research, Office of Basic Energy Sciences.

-
- ¹For a recent review see Ll. Mañosa and A. Planes, *Adv. Solid State Phys.* **40**, 361 (2000).
- ²K. Ullakko, J.K. Huang, C. Kantner, R.C. O'Handley, and V.V. Kokorin, *Appl. Phys. Lett.* **69**, 1966 (1996).
- ³G.H. Wu, C.H. Yu, L.Q. Meng, J.L. Chen, F.M. Yang, S.R. Qi, W.S. Zhan, Z. Wang, Y.F. Zheng, and L.C. Zhao, *Appl. Phys. Lett.* **75**, 2990 (1999).
- ⁴A. Zheludev, S.M. Shapiro, P. Wochner, A. Schwartz, M. Wall, and L.E. Tanner, *Phys. Rev. B* **51**, 11 310 (1995).
- ⁵U. Stühr, P. Vorderwisch, V.V. Kokorin, and P.A. Lindgård, *Phys. Rev. B* **56**, 14 360 (1997).
- ⁶J. Worgull, E. Petti, and J. Trivisonno, *Phys. Rev. B* **54**, 15 695 (1996).
- ⁷Ll. Mañosa, A. González-Comas, E. Obradó, A. Planes, V.A. Chernenko, V.V. Kokorin, and E. Cesari, *Phys. Rev. B* **55**, 11 068 (1997).
- ⁸A. Planes and Ll. Mañosa, in *Solid State Physics*, edited by H. Ehrenreich and F. Spapen (Academic, New York, 2001), p. 159.
- ⁹A. González-Comas, E. Obradó, Ll. Mañosa, A. Planes, V.A. Chernenko, B.J. Hattink, and A. Labarta, *Phys. Rev. B* **60**, 7085 (1999).
- ¹⁰A. Planes, E. Obradó, A. González-Comas, and Ll. Mañosa, *Phys. Rev. Lett.* **79**, 3926 (1997).
- ¹¹A. Zheludev, S.M. Shapiro, P. Wochner, and L.E. Tanner, *Phys. Rev. B* **54**, 15 045 (1996).
- ¹²V.A. Chernenko, *Scr. Mater.* **40**, 523 (1999).
- ¹³A simplified version of this calorimeter is presented in Ll. Mañosa, M. Bou, C. Calles, and A. Cirera, *Am. J. Phys.* **64**, 283 (1996).
- ¹⁴E. Obradó, Ll. Mañosa, and A. Planes, *Phys. Rev. B* **56**, 20 (1997).
- ¹⁵R. Kainuma, H. Nakano, and K. Ishida, *Metall. Mater. Trans. A* **27A**, 4153 (1996).
- ¹⁶J. Pons, V.A. Chernenko, R. Santamarta, and E. Cesari, *Acta Mater.* **48**, 3207 (2000).
- ¹⁷The sample investigated by Zheludev *et al.* is assumed to be stoichiometric because the actual composition is not given.
- ¹⁸U. Stühr, P. Vorderwisch, and V.V. Kokorin, *J. Phys.: Condens. Matter* **12**, 7541 (2000).
- ¹⁹S.M. Shapiro, B.X. Yang, Y. Noda, L.E. Tanner, and D. Schryvers, *Phys. Rev. B* **44**, 9301 (1991).
- ²⁰G.L. Zhao and B.N. Harmon, *Phys. Rev. B* **45**, 2818 (1992).
- ²¹T. Castán, E. Vives, and P.A. Lindgård, *Phys. Rev. B* **60**, 7071 (1999).
- ²²S.M. Shapiro, J.Z. Larese, Y. Noda, S.C. Moss, and L.E. Tanner, *Phys. Rev. Lett.* **57**, 3199 (1986).
- ²³F. Zuo, X. Su, and K.H. Wu, *Phys. Rev. B* **58**, 11 127 (1998).